Journal of The Electrochemical Society, **149** (12) F171-F180 (2002)
0013-4651/2002/149(12)/F171/10/$7.00 © The Electrochemical Society, Inc.

Chemically Bonded Porogens in Methylsilsesquioxane

II. Electrical, Optical, and Mechanical Properties

Agnes M. Padovani,[a,*] Laura Riester,[b] Larry Rhodes,[c] Sue Ann Bidstrup Allen,[a] and Paul A. Kohl[a,,z]**

[a]*School of Chemical Engineering, Georgia Institute of Technology, Atlanta, Georgia 30332-0100, USA*
[b]*Oak Ridge National Laboratory, Oak Ridge, Tennessee 37831-6069*
[c]*Promerus LCC, Brecksville, Ohio 44141, USA*

The electrical, optical, and mechanical properties of porous methylsilsesquioxane (MSQ) films created using two different sacrificial polymers: trimethoxysilyl norbornene (TMSNB), and triethoxysilyl norbornene (TESNB) were evaluated in this study. The introduction of porosity lowered the dielectric constant, the index of refraction, and the elastic modulus and hardness of the films as compared to the nonporous MSQ films. The dielectric constant was lowered from 2.7 for a pure MSQ film to 2.35 for a film with 30 wt % initial concentration of TMSNB. Similarly, the index of refraction was lowered from 1.42 to 1.30 for a 30:70 wt % TMSNB:MSQ film. The TMSNB:MSQ films showed a transition from closed-to-open cell porosity in the range from 20 to 30 wt % loading of sacrificial polymer as determined from positron annihilation spectroscopy. Improvements in the fracture toughness were observed for the TESNB:MSQ films as compared to the pure MSQ or TMSNB:MSQ films.
 [DOI: 10.1149/1.1515282]

Manuscript received March 11, 2002. Available electronically October 16, 2002.

Previous studies have reported on the development and fabrication of porous methylsilsesquioxane (MSQ) films and on the use of trimethoxysilyl norbornene (TMSNB) and triethoxysilyl norbornene (TESNB) as sacrificial polymers for developing porosity within the MSQ matrix.[1,2] It was shown that these polymers decompose cleanly (with minimal residue) upon exposure to elevated temperatures (~425°C), and the decomposition products volatilize and permeate through the MSQ matrix leaving behind pores, thus acting as sacrificial place-holders. Different pore microstructures were observed depending on the sacrificial polymer used to create the films, and the differences were attributed to variations in the chemical interaction between the polymer and the MSQ in the mixtures. Chemical analysis has shown that the TMSNB polymer forms a chemical bond with the MSQ that produces a more uniform distribution of smaller pores (original polymer sites) throughout the matrix, as compared to TESNB, which phase-separates from the MSQ. In Part I of this paper,[2] the chemical structure of the sacrificial polymer/MSQ mixtures was investigated, and the thermal properties of the samples were reported. The goal of this article is to characterize the electrical, optical, and mechanical properties of the porous microstructures obtained from TMSNB and TESNB sacrificial polymers in MSQ.

Experimental

The porous films were prepared, as described previously,[2] using Honeywell 418 MSQ (Santa Clara, CA) as the main polymer matrix and homopolymers of trimethoxysilyl norbornene (TMSNB) and triethoxysilyl norbornene (TESNB) as the sacrificial materials (Promerus LLC, Brecksville, OH). Variations in the molecular weight of the sacrificial polymer were evaluated for both the TMSNB (Mw ~49,000-68,000) and the TESNB (Mw ~ 39,000-58,000). The concentration of sacrificial polymer in the films was also varied from 0-60 wt % in the case of TMSNB, and from 0-30 wt % for the TESNB samples (polymer loads are based on the initial solutions of MSQ with the sacrificial polymers). Solutions of the individual components were prepared in methyl isobutyl ketone (MIBK) prior to mixing in specific ratios to avoid solvent incompatibilities that could induce phase separation upon mixing. The NB:MSQ mixtures were spin-coated onto silicon ⟨100⟩ substrates at different speeds to obtain films of approximately 300-1100 nm in thickness. The thickness was measured using an Alpha-step profilometer after patterning and etching with buffered oxide etch (BOE) selected portions of the films to create step-heights. The cure process applied to these samples consisted of a sequence of hot plate bakes at 180°C for 2 min and at 250°C for 1 min, followed by a furnace cure at 425°C for 1.5 h. The furnace cure was necessary to convert the MSQ into a network structure and to decompose the sacrificial material within the films. The furnace was ramped at 2°C/min to the final temperature, and maintained under a nitrogen atmosphere (flow rate = 35 slpm) to minimize the oxygen content in the chamber and avoid oxidation of the films.

For electrical testing, metal-insulator-metal parallel plate capacitors were fabricated with the porous films. The NB:MSQ mixtures were spin-coated onto metallized silicon wafers. A sputtered Ti/Cu/Ti layer (15/200/15 nm), and patterned aluminum dots (200 nm thick; 1.5 mm diam) served as the bottom and top electrodes, respectively, of the metal-dielectric-metal structures. An HP LCR meter was used to measure the capacitance and conductance of the capacitors at 10 kHz. An average of 60 to 200 capacitors were measured for each dielectric mixture.

A Plasmos ellipsometer with a 632.8 nm wavelength and a 70° angle of incidence was used to measure the index of refraction of the porous films. For these studies, the films were deposited on silicon wafers. Transmission electron microscopy (TEM) was used to evaluate the pore microstructure after decomposition of the sacrificial materials. The resulting pore size and distribution were analyzed from ultrathin cross sections prepared using focused ion beam etching. Atomic force microscopy (AFM) was performed to characterize the surface topography of the porous films. The AFM images were recorded with a Nanoscope IIIa from Digital Instruments, Inc. Silicon cantilevers in the tapping mode were used to avoid deformation or indentation of the sample surfaces by the tip. To study the pore interconnectivity within the films, positron annihilation spectroscopy (PAS) experiments were performed. A combination of the Doppler broadening and 3-photon positronium decay techniques was used to calculate the escape length of positronium species from the porous films. The moisture uptake of the porous films was measured with a quartz crystal nanobalance (model EQCN-701 from Elchema, Inc.). Moisture absorption data was recorded as a function of the loading of the sacrificial polymer in the films, and under various humidity conditions (range of ~20 to 98% RH). For these studies, the NB:MSQ mixtures were deposited on quartz crystals with prefabricated gold electrodes. All the experiments were conducted at room temperature.

Nanoindentation experiments were conducted to evaluate the mechanical properties of the porous dielectric films using a Nano Indenter II by Nano-Instruments, Inc. (Oak Ridge, TN). The elastic

* Electrochemical Society Student Memeber.
** Electrochemical Society Active Member.
z E-mail: paul.kohl@che.gatech.edu

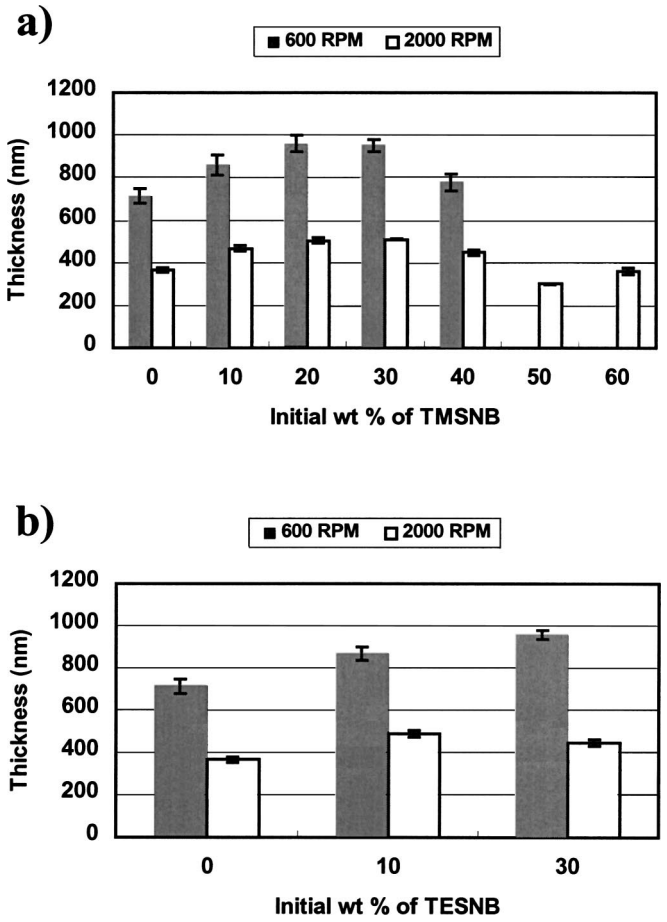

Figure 1. Spin curves for the (a) TMSNB and (b) TESNB polymer systems showing the final thickness (after cure and decomposition) as a function of the load of sacrificial material in the film.

modulus and the hardness were calculated from the data for the hold segments of a continuous stiffness experiment based on the method described by Oliver *et al.*[3] A total of ten indents per sample were made with each consisting of three penetration-hold segments. The penetration depths were fixed at 25, 50, and 75 nm in order to avoid the effect of the underlying silicon substrate on the measurements. Fused silica was used as the calibration standard for these measurements. To evaluate the fracture toughness, or the resistance to crack propagation in the films, a different experiment was performed using a cube-corner tip geometry. For this study, five indents at each of six different loads were made per sample. For the TESNB samples, the range of applied loads varied from 0.01 to 10 mN. The loads were varied from 0.25 to 5 mN for films made with TMSNB as the sacrificial material. Different thickness ranges were evaluated for both sacrificial systems. Crack-free areas were chosen for performing the tests. After the indentation process, scanning electron microscopy (SEM) was used to measure the length of the cracks propagating from the corners of the impressions. These measurements were taken within a relatively short time after the indents were made, so that negligible crack growth could be assumed.

Results

Figures 1a and b show spin-speed curves for the TMSNB and TESNB sacrificial systems in MSQ, respectively. Thickness values, measured after cure and decomposition of the sacrificial materials, are reported as a function of the loading of the sacrificial polymer and the spin speed used to prepare the films. For TMSNB, the thickness increases with the concentration of sacrificial polymer in the film up to about 30 wt %, and then slightly decreases at higher concentrations. At the higher loadings, a considerable amount of material is eliminated upon heating, thereby resulting in thinner films.

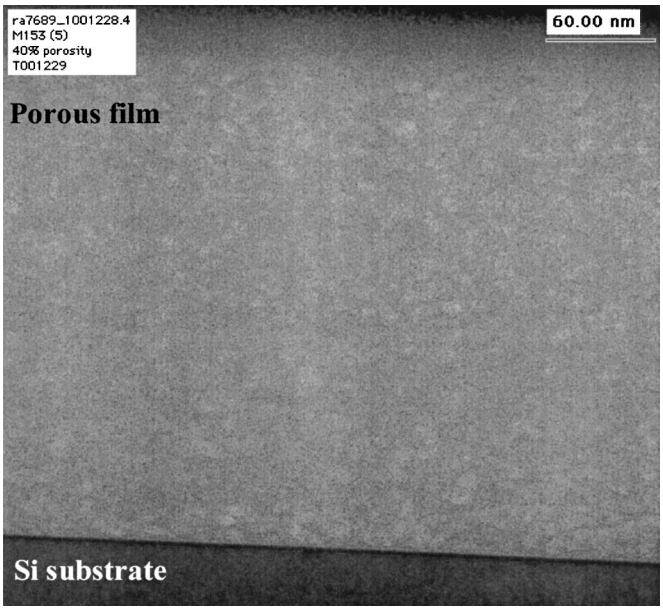

Figure 2. TEM micrograph for a 40:60 wt % TMSNB:MSQ film after decomposition of the sacrificial material at 425°C.

Porosity characterization: TEM, AFM, and PAS studies.—Figure 2 shows a TEM cross section of a 40:60 wt % TMSNB:MSQ film after decomposition of the sacrificial polymer (TMSNB Mw = 57,000). The light regions in the image correspond to the porosity (less electron-dense areas), which appears to be uniformly distributed throughout the MSQ matrix (no agglomeration was observed at the surface of the film or at the interface with the silicon substrate). The micrograph shows nanosize pores on the order of ~3 to 10 nm within the bulk of the dielectric film. However, little else can be inferred regarding the pore distribution due to the lack of depth resolution. In previous TEM studies,[2] performed as a function of the loading of sacrificial TMSNB in the films, similar results were observed for the 10-30 wt % samples. The average pore size remained the same regardless of the concentration of sacrificial polymer used to prepare the films (in the range from 10-40 wt % TMSNB). However, the density of pores was proportional to the polymer loading in the films. In Part I of this study,[2] it was shown that chemical bonding between the sacrificial polymer and MSQ matrix mitigated the problems with phase segregation and provided uniform distribution of nano-size pores in the TMSNB:MSQ films. However, higher concentrations of TMSNB (*i.e.*, greater than 40 wt %) did not result in nanoporous films. TEM images of 50:50 and 60:40 wt % TMSNB:MSQ films reveal very few pores within the bulk of the films. AFM studies performed on these samples did not show any characteristic topography or pore-resembling patterns on the surface of the films. Therefore, the combination of TEM and AFM observations on these TMSNB:MSQ films suggest that, even if some degree of phase separation occurred in the TMSNB blends due to insufficient reaction with the MSQ matrix, the polymer was still miscible with the MSQ.

Previous TEM and AFM studies performed with the TESNB:MSQ films have demonstrated the lack of nanoporosity within the bulk of the films and the evolution of characteristic surface cavities upon decomposition of the sacrificial material.[2] In this paper, the surface morphology was studied as a function of the loading of sacrificial polymer (Mw = 39,000) in the films. Figures 3a and b show the AFM and TEM results, respectively, for a 10:90 wt % TESNB:MSQ film after decomposition of the TESNB. Figure

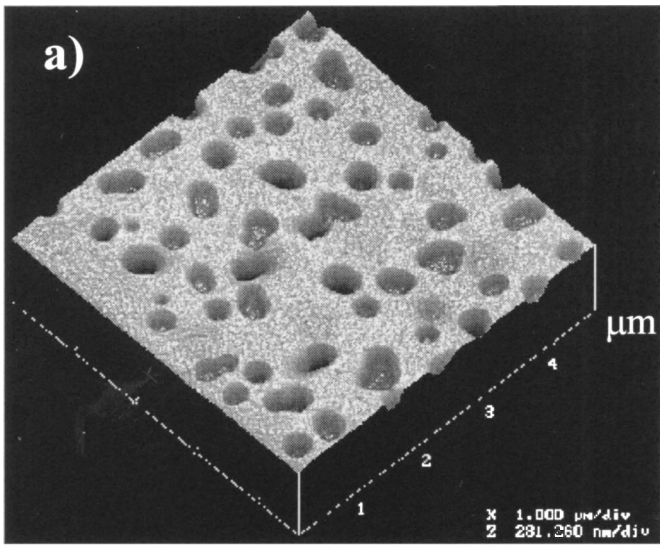

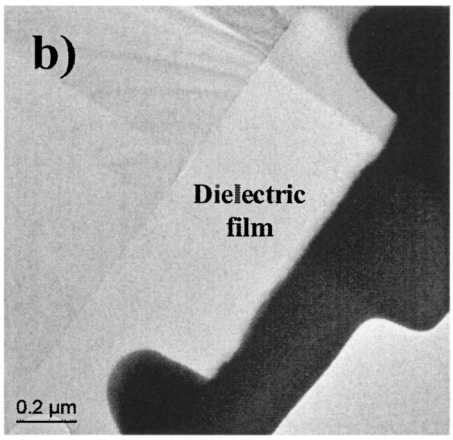

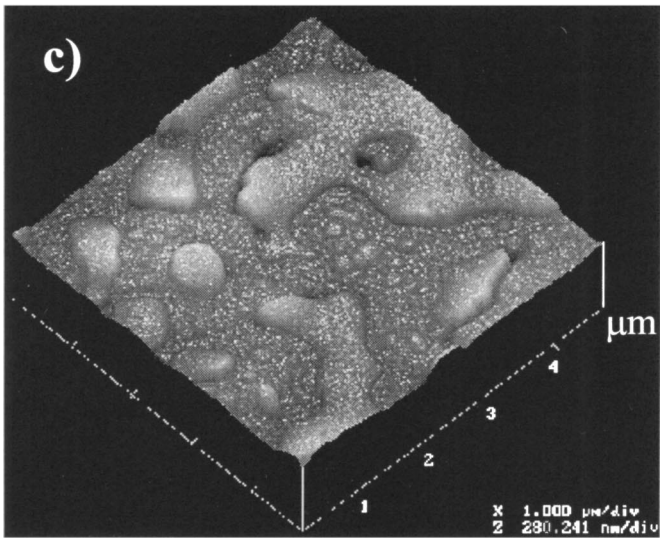

Figure 3. (a) AFM and (b) TEM images for a 10:90 wt % TESNB:MSQ film, and (c) AFM image for a 20:80 wt % TESNB:MSQ sample after decomposition of the sacrificial polymer.

3c shows the corresponding AFM image for a 20:80 wt % TESNB:MSQ sample. The AFM image for the film with 10 wt % TESNB concentration shows cavities on the surface with diameters of ~300 nm. The TEM micrograph shows a nonporous, amorphous film very much like pure MSQ with dimples on the surface that

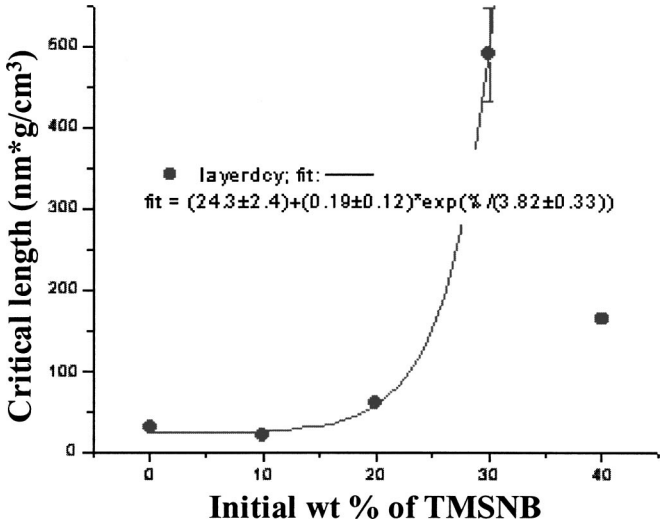

Figure 4. Results for the pore connectivity studies of TMSNB:MSQ films as determined from positron annihilation spectroscopy.

extend approximately half-way into the dielectric layer. Based on these observations, it can be concluded that the surface cavities are the only pores formed in the film upon exposure of the TESNB to the decomposition temperature. Increasing the amount of sacrificial TESNB in the films creates larger surface cavity domains (on the order of micrometers) and nonuniform surface morphologies as shown in Fig. 3c for 20 wt % loading of the TESNB polymer.

One of the critical limitations for the use of porous materials as interlevel dielectrics is the inability to create films with closed nanoporosity. In this regard, positron annihilation spectroscopy studies were conducted to investigate the pore connectivity within the films. Figure 4 shows the results of the PAS experiments for the TMSNB:MSQ samples after heat-treatment at 425°C. The escape depth of the positronium species from the porous matrix is plotted as a function of the loading of sacrificial TMSNB (Mw = 57,000) used to prepare the films. It has been suggested that the values for the escape depth in the films would correlate with the average size of the pore clusters connected to the surface, assuming the clusters were homogeneously and isotropically distributed throughout the film.[4] The escape depth was calculated from the doppler broadening parameters (S and W) and the three-photon signal, which is dependent on void size and density, therefore the units: nm g/cm^3.[5] Based on Fig. 4, the calculated escape depth for the 20 wt % TMSNB film is 24 nm g/cm^3, which is approximately the same as the value obtained for the nonporous MSQ sample (0 wt % TMSNB). However, the escape depth for the 30 wt % film was calculated as 490 ($\pm$50) nm g/cm^3. The dramatic increase in escape depth between 20 and 30 wt % loading of TMSNB indicates the transition from closed to open-cell porosity. Therefore, the results show that the samples with 10 and 20 wt % concentration of TMSNB have closed-cell porosity, while the 30 and 40 wt % samples have open porosity, or a fully connected porous microstructure. The 40:60 wt % TMSNB:MSQ sample, however, showed a lower escape depth than the 30:70 wt % film, which suggests that the pore channels in this sample extend all the way across the film to the interface with the silicon substrate. At the film/substrate interface, the possibility for pick-off annihilation increases dramatically and causes a loss of the 3-photon signal, which consequently decreases the escape depth calculated for the film.[4] Further studies are required to determine the density, and therefore, the absolute escape depth for the films. Knowledge of the dimensions of the pore cavities could aid in understanding the reasons for interconnected microstructures being observed at polymer loads which are unlikely to have crossed the percolation threshold. Similar studies were not conducted with the TESNB:MSQ mixtures

Table I. Moisture absorption results for TMSNB:MSQ films after cure at 425°C as a function of the load of sacrificial polymer in the mixtures. Experiments conducted at room temperature and 85% relative humidity.

Concentration of TMSNB (wt %)	Moisture absorption (wt % H_2O)
0	0.170
10	0.194
20	0.208
30	0.245
40	0.279

because they were not found to possess nanometer-size pores within the bulk of the films.

Moisture absorption studies.—Table I shows the results of the moisture absorption experiments performed on TMSNB:MSQ samples after heat-treatment at 425°C. The average weight percent of water absorbed at a relative humidity (RH) of 85% is shown as a function of the loading of TMSNB polymer used to prepare the films. The results show that, under these humidity conditions, a pure MSQ film absorbs approximately 0.170 wt % of water, whereas films with 10 and 40 wt % TMSNB absorb 0.194 and 0.279 wt % H_2O, respectively. These results exhibit a near-linear increase in the water uptake with the concentration of sacrificial polymer in the film. Similar studies conducted with TESNB:MSQ mixtures resulted in a 0.503% of water absorbed for a film containing 10 wt % TESNB, which is significantly higher ($\sim$2.5 times) compared to the equivalent TMSNB film. The higher moisture absorption in the TESNB films is attributed to the surface cavities, developed during the decomposition of the sacrificial polymer, which provide a large surface area for water adsorption and subsequent diffusion into the film. In comparison, a significant fraction of the nanosize pores in the 10:90 wt % TMSNB:MSQ film are closed, thereby limiting the surface area exposed for water adsorption.

Electrical properties.—The relative permittivity (ε', real part of the complex dielectric constant) of the porous films was calculated using the equation, $\varepsilon' = Ct/\varepsilon_0 A$, which relates the permittivity of the dielectric material to the capacitance (C), the thickness (t) of the film, and the area (A) of the electrode in a parallel-plate capacitor structure (ε_0) is the permittivity of free space.[6] Only defect-free capacitors with low conductance, typically below 0.01 μS, were used to calculate the results. Therefore, the relative permittivity is approximately the same as the dielectric constant within the two significant figures reported. A correction for the fringing fields around the perimeter of the capacitors was made, according to the formula given in Ref. 6 for structures with unequal electrodes, even though it was considerably small ($\sim$0.008) in this case. Figure 5 shows the dielectric constant for the TMSNB:MSQ samples after heat-treatment at 425°C as a function of the initial concentration of sacrificial polymer (Mw = 57,000) in the film. The measured dielectric constant of 2.69 for pure MSQ (0 wt % TMSNB in Fig. 5) agrees well with the reported value of 2.7 at 1 MHz.[7] The results show an average dielectric constant of 2.41 ± 0.12, 2.32 ± 0.09, 2.35 ± 0.28, and 2.34 ± 0.43 for TMSNB concentrations of 10, 20, 30, and 40 wt %, respectively. The rather large standard deviations observed in the values for the 30 and 40 wt % TMSNB loadings suggest the presence of considerable film nonuniformities in the samples. Also shown in Fig. 5 are the expected values of the dielectric constant of porous films based on the Maxwell-Garnett theory,[8,9] a model developed by Jayasundere *et al.*[10] for binary piezoelectric composites, and the logarithmic mixture rule used by Xu *et al.*[11] to study the dielectric constant of a porous poly(arylether) material. The values for the models were calculated using the estimated volume fractions of the individual components in the mixtures. All the models show the trend of decreasing dielectric constant with loading

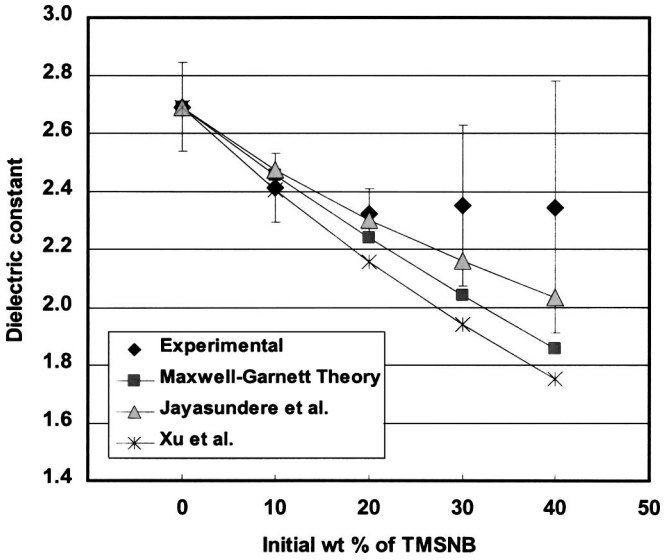

Figure 5. Dielectric constant for TMSNB:MSQ mixtures after cure and decomposition as a function of the initial concentration of sacrificial polymer in the films and comparison with theoretical models for the dielectric constant of porous films.

of sacrificial polymer in the films, as expected for the introduction of air upon development of porosity. The experimental results for the TMSNB:MSQ samples agree with predicted values at polymer loadings of 20 wt % or less. The measured dielectric constants for the 10 and 20 wt % TMSNB films differ only by 1.8 and 3.7%, respectively, from the Maxwell-Garnett theory. A greater deviation from the three models is observed for the 30 and 40 wt % TMSNB samples. It was not possible to measure the dielectric constant for the TESNB:MSQ mixtures due to the surface cavities.

Optical properties.—Table II shows the index of refraction data for a set of TMSNB:MSQ films after heat-treatment at 425°C for 1.5 h. The average index for a pure MSQ film was 1.42, which differs from the literature value of 1.36 by 4.4%.[7] The difference is probably within experimental error (from the instrument and the average thickness of the film used to estimate the index of refraction). The results show a decreasing trend in the index of refraction of the films in the range from 0 to 30 wt % TMSNB. For the 10:90 wt % TMSNB:MSQ film, the average index of refraction was 1.35, while an index of refraction of 1.30 was measured for the film with 30 wt % sacrificial polymer (Table II). In comparison, the predicted values

Table II. Index of refraction data for TMSNB:MSQ films before and after heat-treatment at 425°C as a function of the initial concentration of sacrificial polymer used to prepare the films.

Polymer loading (wt %)	Index of refraction		
	Before cure	After cure (1.5 h)	After cure (5 h)
	TMSNB Mw = 57,000		
0		1.42 ± 0.01	
10		1.35 ± 0.01	
20		1.32 ± 0.01	
30		1.30 ± 0.02	
40	1.47 ± 0.05	1.34 ± 0.01	1.34 ± 0.01
50	1.37 ± 0.02	1.35 ± 0.03	
60	1.37 ± 0.08	1.40 ± 0.01	
	TMSNB Mw = 46,550		
30	1.45 ± 0.02	1.30 ± 0.01	
	TMSNB Mw = 67,450		
30	1.46 ± 0.01	1.31 ± 0.01	

from a linear mixing rule in the index of refraction (based on the estimated volume fractions of the individual components) are 1.37 and 1.28 for the 10 and 30 wt % sacrificial polymer loadings, respectively. Based on these values, the results show a 1.5 and 1.7% difference between the estimated and experimental values for the 10:90 and 30:70 wt % TMSNB:MSQ films, respectively. In the range from 40 to 60 wt % TMSNB concentration, the index of refraction increases, and the value of 1.40 measured at 60 wt % polymer loading is close to that for pure MSQ. In the case of the TESNB:MSQ samples, the surface cavities prevented the measurement of reliable data for the index of refraction of the films.

To evaluate the increase in index of refraction with TMSNB polymer concentration above 30 wt %, index measurements were taken as a function of the cure process. The index of refraction was measured for 50:50 and 60:40 wt % TMSNB:MSQ films before cure (after heat-treatment at 180°C for 2 min) and after cure at 425°C for 1.5 h, and for a 40:60 wt % TMSNB:MSQ film after heat-treatments at 425°C for 1.5 and 5 h to determine the effect of cure time (data also shown in Table II). For the 50:50 wt % TMSNB:MSQ film, the average index of refraction changes from 1.37 before cure to 1.35 after cure, and similarly, the index of refraction for the 60:40 wt % TMSNB:MSQ film also lowers upon curing. These reductions, however, only approach the value for pure MSQ. In the case of the 40:60 wt % sample exposed to different cure times, the index of refraction does not show any variations with time, which suggests that the standard 1.5 h cure time allows sufficient time for the TMSNB polymer to decompose within the film and for the degradation products to permeate through the MSQ matrix.

The index of refraction was measured as a function of the molecular weight of the TMSNB polymer used to prepare the films (refer to Table II). Three different 30:70 wt % TMSNB:MSQ films were prepared with polymer molecular weights in the range from 49,550 to 67,450, and the index of refraction was measured before and after cure at 425°C for 1.5 h. For the three samples, the average index of refraction was ~1.45 before cure, and 1.30 after cure, thereby showing that the index of refraction is approximately the same regardless of the molecular weight of the polymer, at least within the narrow range studied in this case. Further characterization is required to determine the effects of molecular weight on other film properties, especially the porous microstructure, since a previous report[12] showed pores of ~70 nm in diameter with a polymer molecular weight of ~180,000 (as opposed to the ~3 to 10 nm with Mw = 57,000 shown in this study).

Mechanical characterization: elastic modulus and hardness.—The elastic modulus and the hardness of the porous films were evaluated using a method similar to the one described by Oliver *et al.*[3] The mechanical properties were calculated from load *vs.* displacement data obtained from nanoindentation experiments in a continuous stiffness mode. The elastic modulus (E) for the films was determined from Eq. 1

$$\frac{1}{E_r} = \frac{(1 - \upsilon^2)}{E} + \frac{(1 - \upsilon_i^2)}{E_i} \qquad [1]$$

where υ is the Poisson's ratio for the material, E_i (1141 GPa) and υ_i (0.07) are the elastic modulus and Poisson's ratio for the indenter, respectively, and E_r is the reduced modulus obtained from Eq. 2

$$E_r = \frac{S\sqrt{\pi}}{2\beta\sqrt{A}} \qquad [2]$$

In Eq. 2, S is the elastic stiffness or the slope of the unloaded curve at the beginning of the unloading segment when only elastic recovery is involved, β is a correction factor dependent on the tip geometry, and A is the area of contact.[13] For the Berkovich tip used in these experiments, the β factor is 1.034. The area of contact was calculated from the calibrated or experimentally determined tip area function, which relates the plastic or contact depth with the tip geometry. The hardness was calculated from the peak indentation load (P) and the area of contact ($H = P/A$).

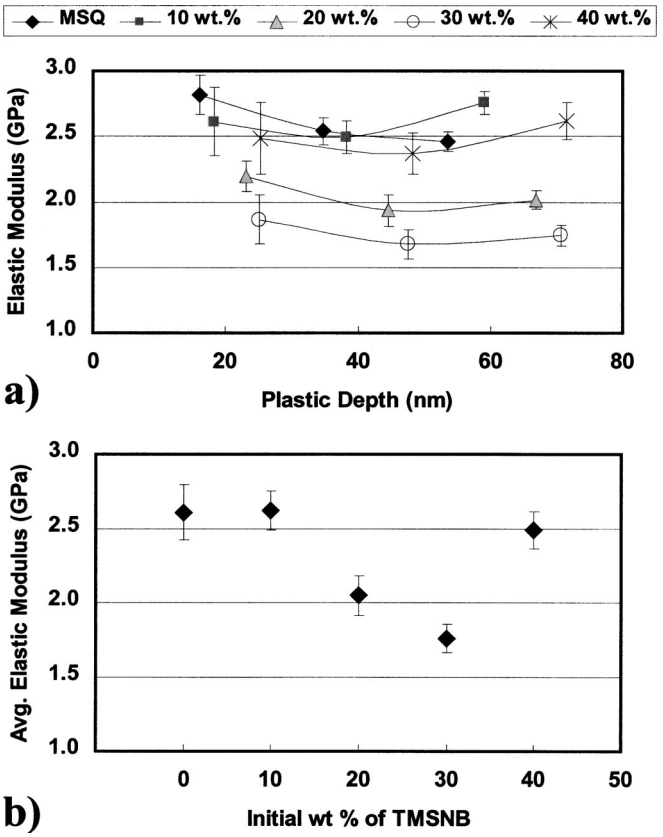

Figure 6. Plot of the (a) elastic modulus as a function of the calculated plastic depth, and (b) the average elastic modulus as a function of the concentration of sacrificial polymer in the films for a set of TMSNB:MSQ films after heat-treatment at 425°C for 1.5 h.

Figures 6 and 7 show the results for the mechanical properties of TMSNB:MSQ films after cure at 425°C for 1.5 h (film thickness ~400 to 600 nm; TMSNB Mw = 57,000). Figures 6a and 7a show the results for the elastic modulus and the hardness, respectively, as a function of the plastic depth and the concentration of TMSNB in the films. The plastic depth was determined from the difference between the total depth, or the displacement of the indenter into the film, and the depth of the surface after the load was removed. The results for the modulus (Fig. 6a) show similar trends in the data as a function of depth, with slightly higher values measured at the lowest penetration (~25 nm displacement). However, for the same indentation procedure, the indents for the 30:70 and 40:60 wt % TMSNB:MSQ samples show larger plastic depths. These samples also show the largest standard deviation in the results at the three plastic depths measured (15 data points collected at each penetration depth). As a function of the concentration of TMSNB in the films, the results show a decrease in the elastic modulus with concentration, except for the 40 wt % sample, in which case, the fully-connected porous microstructure in the film made the sample appear less compliant probably due to mechanical failure during testing. Similar results were observed in the hardness plot (Fig. 7a). The hardness of the porous films seems to be independent of the plastic depth at which it was measured, and it also decreases with concentration of TMSNB in the films, except for the 40 wt % sample, which similarly does not follow the trend of the lower polymer loads. Figures 6b and 7b show the average elastic modulus and hardness, respectively, as a function of the initial concentration of TMSNB in the films. For a pure MSQ film (0 wt % TMSNB), the

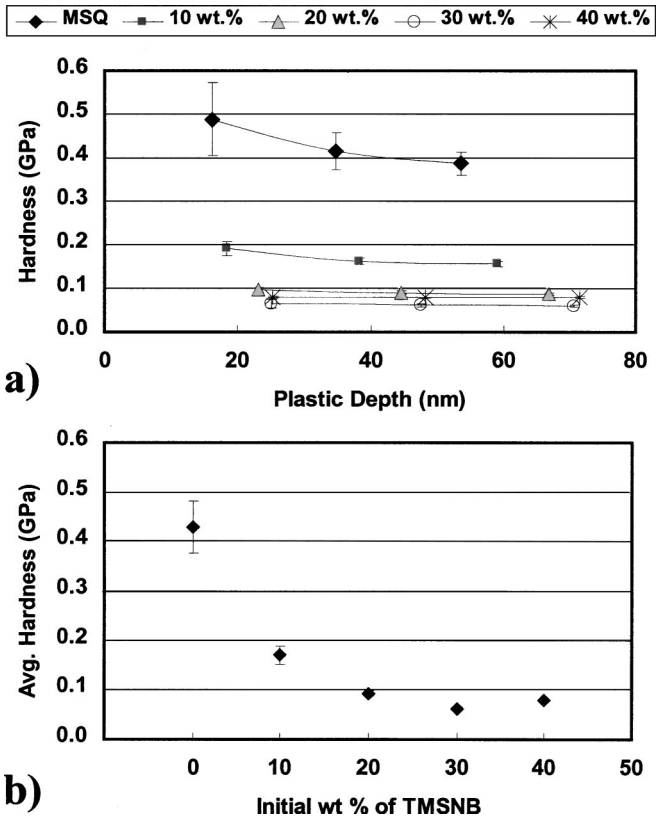

Figure 7. Plot of the (a) hardness as a function of the calculated plastic depth, and (b) the average hardness as a function of the concentration of sacrificial polymer used to prepare the films for a set of TMSNB:MSQ films after heat-treatment at 425°C for 1.5 h.

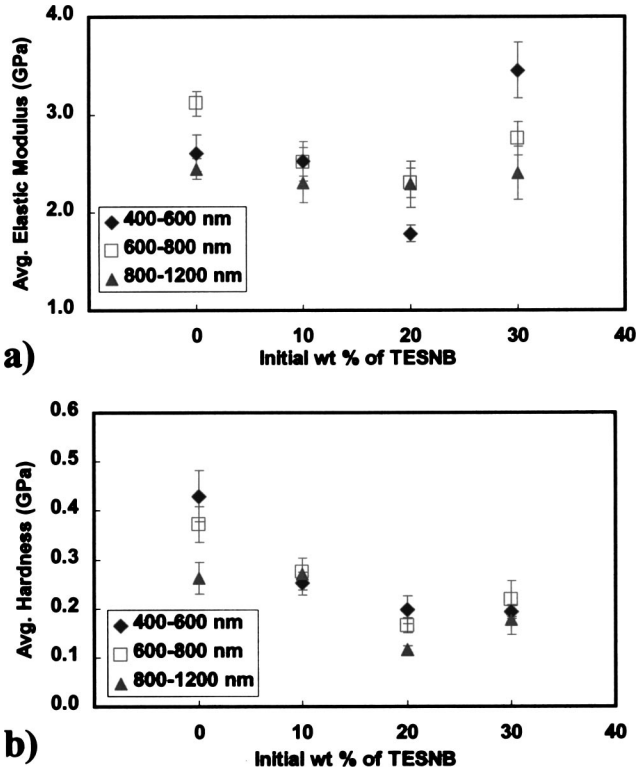

Figure 8. Plot of the average (a) elastic modulus and (b) hardness of TMSNB:MSQ films after cure at 425°C as a function of the load of sacrificial polymer in the films and the thickness of the films.

average elastic modulus measured was 2.6 (±0.2) GPa, and the hardness was 0.43 (±0.05) GPa. The results for the elastic modulus of MSQ are comparable, within experimental error, to the literature value of 3.2 GPa. However, the measured hardness was slightly lower than the reported value of 0.7 GPa for pure MSQ.[14] Both mechanical properties decrease with concentration of TMSNB (at least in the range 0-30 wt %), and the average results for a 30:70 wt % TMSNB:MSQ film show an elastic modulus of 1.8 GPa and a hardness of 0.06 GPa, which are about an order of magnitude higher as compared to similar aerogel films with 20 nm pores.[15]

Nanoindentation experiments performed with similar TESNB:MSQ films (TESNB Mw = 58,000) resulted in comparable mechanical properties to those measured for the TMSNB system. For the 10:90 and 30:70 wt % TESNB:MSQ films, the average elastic modulus was 2.4 and 1.3 GPa, respectively. The average hardness for the same films was 0.18 and 0.08 GPa, which are similar to the 10:90 and 30:70 wt % TMSNB:MSQ films at 0.17 and 0.06 GPa, respectively. Even though the differences in porosity microstructure obtained with the two sacrificial polymers did not affect the mechanical properties of the films, significant differences were observed in terms of the reproducibility of the results. Larger scattering was observed in the data for the TESNB samples.

Figure 8 shows the average (a) elastic modulus and (b) hardness for TESNB:MSQ films after cure at 425°C as a function of the concentration of TESNB used to prepare the films and the thickness of the films. The results show a near-linear decrease in the mechanical properties with concentration of TESNB in the films, except for the 30 wt % sample, which was the least reproducible sample in terms of the measured values for the elastic modulus. The properties show minimal dependence on the thickness of the films, as was expected, since the experimental design allowed maximum film penetrations of 75 nm in order to avoid any substrate effects. Pure MSQ films were thinner than the porous films, so these results could have been affected by the underlying silicon substrate (Si properties: E = 185.6 GPa, H = 11.5 GPa.[16]

Mechanical properties: fracture toughness.—The fracture toughness (K_c), or the resistance to crack propagation, was also evaluated for the porous TMSNB and TESNB:MSQ films. A method similar to the one described by Harding *et al.*[17] was used to test the films, and the fracture toughness was calculated from Eq. 3 developed by Lawn *et al.*[18]

$$K_c = \alpha\left(\frac{E}{H}\right)^{1/2}\left(\frac{P}{c^{3/2}}\right) \qquad [3]$$

Where α is an empirical constant dependent on the tip geometry (0.036 for cube-corner), E is the elastic modulus, H is the hardness, P is the applied load, and c is the length of the radial cracks propagating from the corners of the indentation impressions. Figure 9 shows SEM images of the typical indentation arrays used to test the fracture toughness of the films. Figure 9a corresponds to a sample of pure MSQ and Fig. 9b and c show the indents for two 10:90 wt % samples of TESNB and TMSNB:MSQ, respectively. The average thickness of the MSQ film was 714 nm, and the two porous films had a thickness of ~860 nm. Figure 9 shows indents at 5, 1.5, 1.0, 0.75, 0.5, and 0.25 mN force (left to right), with five repetitions at each applied load shown from top to bottom. Therefore, each sample shows a total of 30 indents. The range of applied loads was determined from preliminary studies with TESNB:MSQ mixtures, which showed the cracking threshold for the films to be above 0.1 mN force (at 0.1 mN the indents were totally elastic). Even though the same indentation pattern was applied to the samples, significantly different results were observed with the two polymer systems for the same concentration of sacrificial material in the films. The TMSNB:MSQ sample shows a highly cracked film with primary cracks on the order of 50 μm for the 5 mN indents (some of the

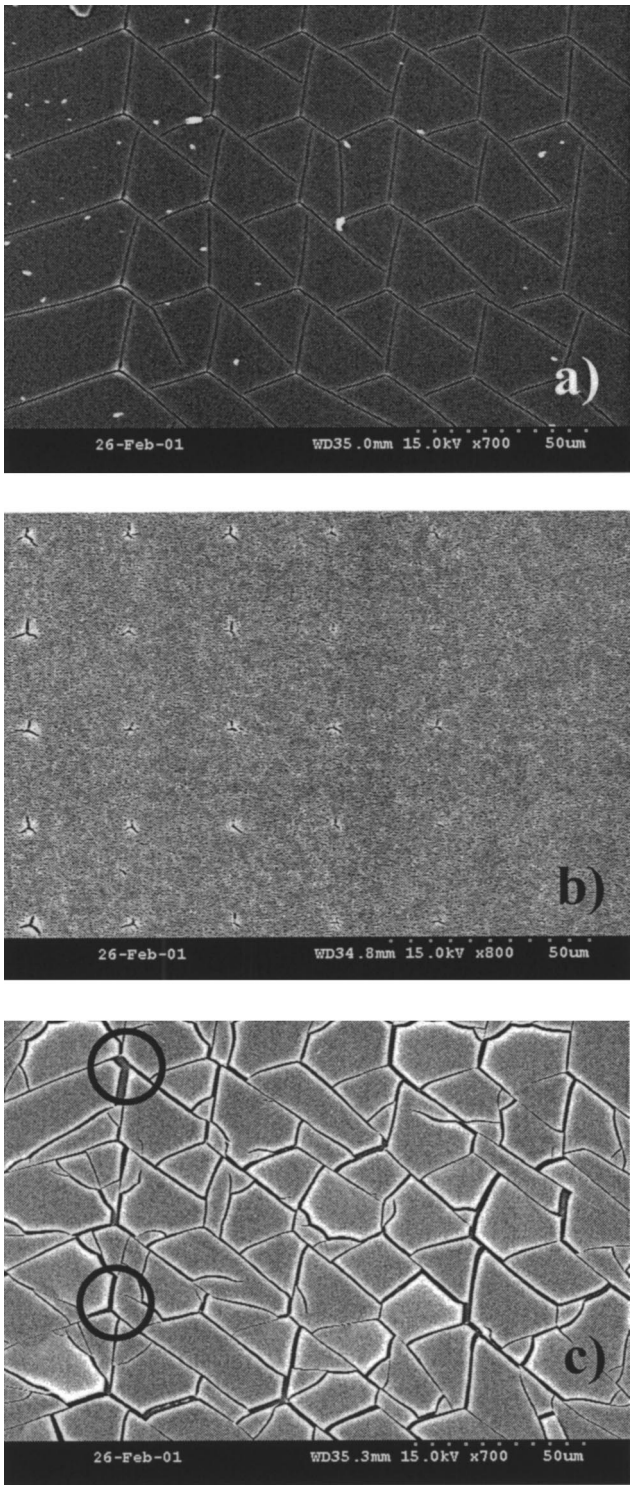

Figure 9. SEM images showing the fracture toughness indents made on a (a) pure MSQ film, (b) a 10:90 wt % TMSNB:MSQ film, and (c) a 10:90 wt % TMSNB:MSQ film. Circled areas denote primary crack extension.

primary cracks were labeled for clarity). On the contrary, minimal crack propagation was observed in the TESNB:MSQ film, which shows cracks of only around 3 μm for the same 5 mN indents. The pure MSQ film also shows extensive cracking (40 μm cracks for 5 mN indents), but not to the degree observed in the TMSNB:MSQ sample (no secondary cracks observed in MSQ).

Figure 10 shows the fracture toughness, calculated from the data for indents made with an applied load of 0.96 mN, for a set of

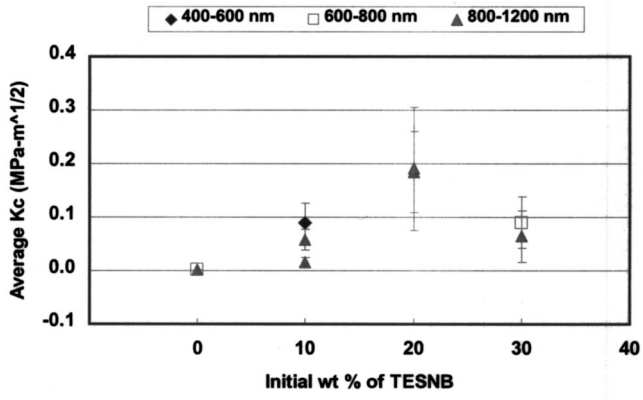

Figure 10. Plot of the average fracture toughness of TMSNB:MSQ films after heat-treatment at 425°C as a function of the initial concentration of sacrificial polymer and the thickness of the films. Data obtained from indents made with an applied load of 0.96 mN.

TESNB:MSQ films after cure at 425°C as a function of the initial concentration of polymer (Mw = 39,000) and the thickness of the films. For the thickness range of 800-1200 nm, the calculated K_c for MSQ was 0.002 MPa-$m^{1/2}$, and the values of 0.06 and 0.19 MPa-$m^{1/2}$ were obtained for polymer loads of 10 and 20 wt % TESNB, respectively. Therefore, the results show about an order of magnitude improvement in the fracture toughness of the films made with TESNB as the sacrificial material. The 30 wt % sample, however, does not show further improvement in the fracture toughness of the films. Even though the penetration (under the same applied load) varied according to the thickness of the films, negligible differences were observed in the K_c values with thickness. Similar results were observed for the fracture toughness regardless of the molecular weight of the TESNB polymer used to prepare the films (as compared to the results with Mw = 58,000).

Figure 11 shows the results for similar studies performed with TMSNB:MSQ mixtures. In this case, the fracture toughness was calculated for indents made with an applied load of 0.72 mN, and the results are shown as a function of the concentration of TMSNB (Mw = 57,000) in the films in the range from 0 to 40 wt %. Overall, very slight improvements, almost negligible within experimental error, were seen in the fracture toughness of the porous TMSNB

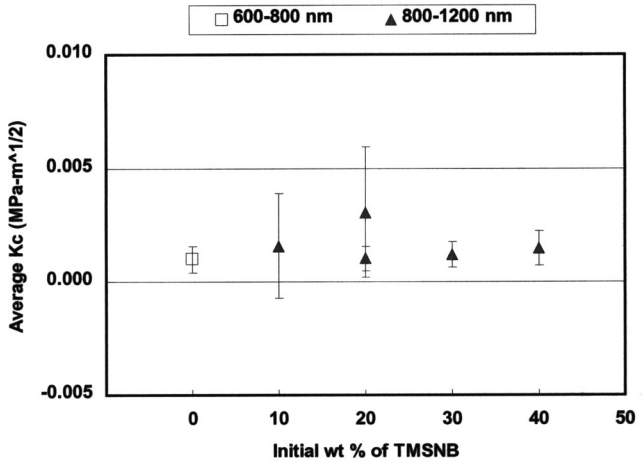

Figure 11. Plot of the average fracture toughness of TMSNB:MSQ films after cure at 425°C as a function of the concentration of TMSNB in the films and calculated from indentation data obtained with an applied load of 0.72 mN.

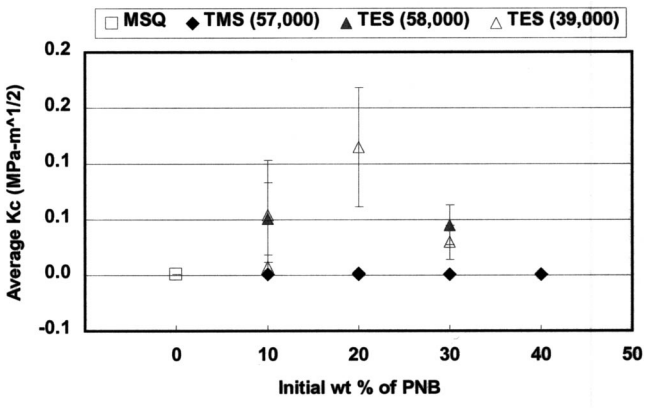

Figure 12. Average fracture toughness for TESNB and TMSNB:MSQ films as a function of the initial concentration of NB in the films and the molecular weight of the sacrificial polymer used. Data obtained from indents made at 0.46 mN applied load.

films as compared to the resistance to cracking of the pure MSQ samples. However, a K_c of 0.001 MPa-m$^{1/2}$ was obtained for a 700 nm thick MSQ film, whereas the K_c value of 0.002 MPa-m$^{1/2}$ was measured for a 10:90 wt % TMSNB:MSQ film with thickness of 860 nm. Also, a 1.1 μm thick film prepared with 20 wt % TMSNB showed a fracture toughness of 0.003 MPa-m$^{1/2}$. Therefore, similar K_c results were obtained, but for slightly thicker films in the case of the porous TMSNB samples as compared to pure MSQ films. The large deviations observed in the fracture toughness of the porous TMSNB:MSQ films are probably due to difficulties in measuring the primary radial cracks because of the interference with secondary cracks.

Finally, the quantitative difference between the two sacrificial systems in terms of the fracture toughness of the films can be observed in the plot shown in Fig. 12. The data compares the average fracture toughness for TESNB and TMSNB:MSQ films as calculated from indentation data at 0.46 applied load, and for films with thickness of 800-1200 nm. The results are shown as a function of the initial weight percent of NB in the films and the molecular weight of the sacrificial polymer used to prepare the films. At 10 wt % polymer concentration, the TESNB:MSQ sample shows a K_c of 0.05 MPa-m$^{1/2}$, and the TMSNB:MSQ film shows a value of 0.001 MPa-m$^{1/2}$. In general, the TESNB:MSQ films show about an order of magnitude improvement in the fracture toughness over the pure MSQ films and the TMSNB:MSQ samples. For both sacrificial systems, the fracture toughness was found to be independent of the load used to make the indents regardless of the penetration into the film.

Discussion

The positron annihilation spectroscopy (PAS) studies performed with the TMSNB:MSQ films revealed critical characteristics of the pore microstructure in the dielectric films. The films showed a transition from closed-to-open cell porosity in the range from 20 to 30 wt % loading of the sacrificial polymer. Based on previous investigations, the closed-cell pore distribution below 20 wt % TMSNB concentration was attributed to the excellent miscibility of TMSNB in MSQ, arising as a result of the reaction of the methoxysilyl moities with the silanol groups in the MSQ matrix (reaction prevents phase segregation of the sacrificial polymer). Furthermore, the measured pore size of 3 nm corresponds to the volume of one TMSNB polymer chain, indicating that there was no significant agglomeration or cross-linking of the polymer with itself, and that the dominating effect on the pore distribution was indeed the reaction of the TMSNB with the MSQ matrix.

However, as the concentration of TMSNB in the MSQ blends is increased, there exists a critical loading threshold beyond which the fraction of TMSNB chains agglomerating and bonding with itself becomes comparable or higher than the fraction chemically reacting with the MSQ matrix. Under such a scenario, the sacrificial material tends to cross-link and forms relatively large polymer phases in the MSQ matrix, which upon degradation at elevated temperatures, lead to the formation of interconnected porous microstructures. PAS data indicates the formation of such interconnected pores at 30 and 40 wt % TMSNB, with continuous structures extending across the film to the interface in the case of the 40 wt % polymer loading sample.

At polymer loadings higher than the threshold level (50 to 60 wt % TMSNB), significantly larger polymeric phases dispersed through the MSQ matrix form as a result of the increased fraction of polymer cross-linking with itself as opposed to reacting with the MSQ. Consequently, during the cure and decomposition process of the sacrificial polymer, extremely high porosity and much larger pore sizes develop in the host matrix. However, such high levels of porosity and large pore sizes greatly deteriorate the mechanical stability of the MSQ film and eventually lead to pore collapse. The phenomenon of pore collapse has been previously observed with other porous materials.[19,20] The combination of microscopic phase separation and subsequent pore collapse would leave behind an MSQ film with few pores. Indeed, TEM micrographs of the films with 50 and 60 wt % TMSNB concentration do not show any porosity, and the critical limit for porosity development was found in the range between 40 and 50 wt % polymer loading. Also, the thickness of the final 50:50 and 60:40 wt % TMSNB:MSQ films after decomposition at 425°C are smaller as compared to the 10-40 wt % films (Fig. 1a), thus supporting the hypothesis of pore collapse.

The results for the refractive index of the TMSNB:MSQ films are also consistent with the previous hypothesis on the evolution of porosity microstructure in the films. The initial reduction in index of refraction, in the range from 10-30 wt % TMSNB concentration (Table II), corresponds to higher porosity developed in the films upon polymer decomposition. The lower index is due to the introduction of air into the films. Although the TEM results showed a highly porous film for the 40:60 wt % TMSNB:MSQ sample (Fig. 2), the pore clusters extending through the film (as determined from PAS) could have caused some scattering in the ellipsometer light; thus, the measured index does not correspond to the observed porosity. For the 50:50 and 60:40 wt % TMSNB:MSQ films, the refractive index matches that of pure MSQ, which is consistent with the previous hypothesis on pore collapse at high polymer loading levels.

Electrical characterization.—Regarding the dielectric constant measurements for the TMSNB:MSQ films (Fig. 5), several factors could be responsible for the differences between the experimental and predicted values. Amongst the three dielectric models evaluated, the results showed better agreement with the Maxwell-Garnett and the Jayasundere *et al.* models, as compared to the logarithmic mixture rule. However, comparable results between the predicted and experimental values were only observed in the range from 0-20 wt % TMSNB concentration. A possible explanation for the deviations observed with larger polymer loadings could be that the Maxwell-Garnett theory and the model developed by Jayasundere *et al.* assume spherical particles (pores in this case) being uniformly distributed in a host matrix with negligible interaction between the particles. The models neglect the changes in the electric field caused by the interaction between particles. These assumptions, however, are hardly acceptable for the TMSNB:MSQ mixtures, especially in the range from 30 to 40 wt % TMSNB concentration, where the PAS experiments identified a high degree of pore connectivity in the films. Therefore, the dielectric models are more applicable at low concentration of the sacrificial polymer where only closed-cell porosity was observed.

The dielectric constants measured for the 30:70 and 40:60 wt % TMSNB:MSQ samples were also higher than expected based on the degree of nanoporosity observed through TEM analysis. One of the factors that could have affected these results is the high level of pore connectivity detected in the films with the positron spectroscopy studies. The variations in the pore clusters throughout the films

could also be responsible for the large deviations or the wide range of dielectric constants measured for both samples. An interconnected porosity microstructure could induce the diffusion of contaminants or moisture into the films, which would be deleterious for the dielectric constant. Likewise, metal diffusion into the inner cavities during electrode deposition would affect the measured electrode area and the film thickness, and hence, erroneous dielectric constant values would be calculated. The moisture absorption increases the interfacial polarization of the material, and therefore the dielectric constant.[6] The increase in moisture absorption with porosity was observed with the TMSNB:MSQ films (Table I), and constitutes one of the disadvantages of the porous films over pure MSQ. Cured MSQ films tend to be hydrophobic because of the Si—CH_3 bonds in the structure,[21] but the introduction of porosity increases the surface area available for water adsorption. As a result of moisture uptake, the 30 and 40 wt % TMSNB samples would exhibit higher dielectric constants than expected. Another aspect that could have influenced the dielectric constant of the porous TMSNB films is the small amount of residue left after decomposition of the sacrificial material in the films. This residue was previously quantified with TGA studies to be around 9 wt % in the case of the TMSNB polymer after curing at 425°C for 1.5 h.[2] Therefore, as the concentration of sacrificial polymer increases in the sample, the amount of residue becomes more significant and could adversely influence the dielectric constant of the films.

Mechanical characterization.—The elastic modulus and the hardness of the porous films decreased with porosity regardless of the sacrificial material used to prepare the films, as expected due to the introduction of air into the films. However, the reduction in the mechanical properties was only seen in the range from 0-30 wt % polymer concentration in the case of the TMSNB:MSQ films (Fig. 6 and 7), and from 0-20 wt % for the TESNB:MSQ samples (Fig. 8). A possible explanation for the higher elastic modulus measured for the 40:60 wt % TMSNB:MSQ film could be that the indentation process caused some of the porosity to collapse under the applied load, and therefore, the calculated properties do not necessarily match the initial state of the film (in terms of porosity). This is possible since the pore clusters in this film extend across the film into the substrate interface, and especially, since similar phenomena were seen to occur naturally (without an applied load) in samples with slightly higher TMSNB concentration.

Significantly higher values of fracture toughness were seen with the TESNB:MSQ films as compared to the pure MSQ films and the TMSNB:MSQ samples (Fig. 12). Pure MSQ films have a high tendency to crack (sometimes by natural occurrence if the thickness threshold of 600 nm has been exceeded) due to the tensile stress developed in the cured films as a result of the strained angle between the Si-O-Si bonds in the structure (tensile stress ~60 MPa[14]). Therefore, pores in the matrix can cause improvements in the fracture toughness. The higher fracture toughness in the TESNB samples, however, was only observed for the 10:90 and 20:80 wt % TESNB:MSQ films (Fig. 10). TEM analysis of these films showed that the surface cavities extended a considerable distance into the thickness of the films (Fig. 3b), which suggests that they could pose as significant barriers for the propagating cracks. Thus, the surface topography, developed from the decomposition of the TESNB polymer, improved the fracture toughness of the films by providing boundaries or termination points for the extending radial cracks. Other groups have also shown improvements in fracture toughness induced by disruptions in the crack-propagating medium.[22,23] In the case of the 30:70 wt % TESNB:MSQ film, an increase in the size of the surface domains could have reduced the number of pore boundaries and therefore, no further improvements (beyond the 20 wt % film) were observed in the fracture toughness. The TMSNB:MSQ films were different from the TESNB samples, and did not show as great an improvement in fracture toughness.

Conclusions

The electrical, optical, and mechanical properties of the porous films were evaluated as a function of the sacrificial polymer used to prepare the films and the concentration of polymer in the films. The results showed that the dielectric constant and the index of refraction of the TMSNB:MSQ films reduced with increasing porosity in the range from 0-20 wt % TMSNB concentration. A polymer-loading threshold was found around 30 wt % TMSNB concentration for the TMSNB:MSQ mixtures, at which level the cross-linking within the polymer chains became comparable to the degree of cross-condensation with the MSQ matrix, and large polymer areas evolved in the films. This was confirmed with the transition from close to open-cell porosity measured with positron annihilation spectroscopy in the range between 20 and 30 wt % TMSNB concentration. Additional studies are necessary to enhance the degree of reaction between the two components in the mixture in an attempt to delay the transition to open porosity.

In terms of the mechanical properties of the films, the elastic modulus and the hardness were observed to decrease with porosity regardless of the sacrificial polymer used to prepare the films, and the fracture toughness of the TESNB:MSQ films showed significant improvements over the pure MSQ and TMSNB:MSQ films. The differences in the resistance to crack propagation were attributed to the surface cavities in the TESNB films, which act as terminating barriers to the propagating cracks.

Acknowledgments

The contribution of Barbara Tsuie for synthesizing the TMSNB and TESNB sacrificial polymers used in this study is gratefully acknowledged. The authors thank Dr. James Conner (Motorola, Austin, TX) and Doug Blom (Oak Ridge National Laboratory, Oak Ridge, TN) for performing the TEM investigation of the porous films. The authors acknowledge Kenneth Rodbell (IBM T. J. Watson Research Center, Yorktown Heights, NY) for performing the positron annihilation spectroscopy studies. One of us (L.R.) acknowledges the sponsorship of the Assistant Secretary for Energy Efficiency and Renewable Energy, Office of Transportation Technologies, as part of the High Temperature Materials Laboratory User Program, Oak Ridge National Laboratory, Managed by UT-Battelle, LLC, for the U.S. Department of Energy under contract number DE-AC05-00OR22725.

Georgia Institute of Technology assisted in meeting the publication costs of this article.

References

1. A. M. Padovani, L. Rhodes, L. Riester, G. Lohman, B. Tsuie, J. Conner, S. A. Bidstrup Allen, and P. A. Kohl, *Electrochem. Solid-State Lett.*, **4**, F25 (2001).
2. A. M. Padovani, L. Rhodes, S. A. Bidstrup Allen, and P. A. Kohl, *J. Electrochem. Soc.*, **149**, F161 (2002).
3. W. C. Oliver and G. M. Pharr, *J. Mater. Res.*, **7**, 1564 (1992).
4. M. P. Petkov, M. H. Weber, K. G. Lynn, and K. P. Rodbell, *Appl. Phys. Lett.*, **79**, 3884 (2001).
5. M. P. Petkov, M. H. Weber, K. G. Lynn, K. P. Rodbell, and S. A. Cohen, *J. Appl. Phys.*, **86**, 3104 (1999).
6. American Society for Testing and Materials, D150-92, *Standard Test Methods for AC Loss Characteristics and Permittivity (Dielectric Constant) of Solid Electrical Insulating Materials*, Philadelphia, PA (1992).
7. Allied Signal Advanced Microelectronic Materials, *Accuspin T-18 Flowable Spin-On Polymer (SOP)*, product bulletin, Allied Signal, Morristown, NJ (1997).
8. H. Ma, R. Xiao, and P. Sheng, *J. Opt. Soc. Am. B*, **15**, 1022 (1998).
9. J. C. M. Garnett, *Philos. Trans. R. Soc. London*, **15**, 2033 (1982).
10. N. Jayasundere and B. V. Smith, *J. Appl. Phys.*, **73**, 2462 (1993).
11. Y. Xu, Y. Tsai, K. N. Tu, B. Zhao, Q. Z. Liu, M. Brongo, G. T. T. Sheng, and C. H. Tung, *Appl. Phys. Lett.*, **75**, 853 (1999).
12. A. T. Kohl, R. Mimna, R. Shick, L. Rhodes, Z. L. Wang, and P. A. Kohl, *Electrochem. Solid-State Lett.*, **2**, 77 (1999).
13. G. M. Pharr, W. C. Oliver, and F. R. Brotzen, *J. Mater. Res.*, **7**, 613 (1992).
14. R. F. Cook and E. G. Liniger, *J. Electrochem. Soc.*, **146**, 4439 (1999).
15. M. Moner-Girona, A. Roig, E. Molins, E. Martínez, and J. Esteve, *Appl. Phys. Lett.*, **75**, 653 (1999).
16. G. M. Pharr, *Mater. Sci. Eng., A*, **253**, 151 (1998).
17. D. S. Harding, W. C. Oliver, and G. M. Pharr, *Mater. Res. Soc. Symp. Proc.*, **356**, 663 (1995).

18. B. R. Lawn, A. G. Evans, and D. B. Marshall, *J. Am. Ceram. Soc.*, **63**, 574 (1980).
19. J. L. Hedrick, R. D. Miller, C. J. Hawker, K. R. Carter, W. Volksen, D. Y. Yoon, and M. Trollsas, *Adv. Mater.*, **10**, 1049 (1998).
20. J. F. Remenar, C. J. Hawker, J. L. Hedrick, S. M. Kim, R. D. Miller, C. Nguyen, M. Trollsas, and D. Y. Yoon, *Mater. Res. Soc. Symp. Proc.*, **511**, 69 (1998).
21. A. C. Descharles, F. Pires, P. Paillet, and J. L. Leray, *Microelectron. Reliab.*, **39**, 279 (1999).
22. A. G. Evans, S. Williams, and P. W. R. Beaumont, *J. Mater. Sci.*, **20**, 3668 (1985).
23. M. Notomi, K. Kishimoto, T. Shibuya, and T. Koizumi, *J. Appl. Polym. Sci.*, **72**, 435 (1999).